Dalton Transactions

PAPER

View Article Online
View Journal

Cite this: DOI: 10.1039/c7dt03400h

Neuroprotective alpha-cleavage of the human prion protein significantly impacts Cu(II) coordination at its His111 site†

Carolina Sánchez-López,[a] Claudio O. Fernández[b] and Liliana Quintanar *[a]

The cellular prion protein (PrP^C) is a copper binding protein that undergoes post-translational modifications, such as endoproteolytic alpha cleavage, which occurs in the vicinity of the His111 Cu binding site. Alpha cleavage processing of PrP^C is considered to be neuroprotective since the cleavage site is located in a region that is key to the conversion of PrP^C into the infectious scrapie isoform (PrP^{Sc}), yielding a membrane bound C1 fragment of PrP^C that still contains His111. In this work, we use hPrP(111–115) fragment as a model peptide to evaluate the impact of alpha cleavage processing of PrP^C in its ability to coordinate Cu(II) ions at His111. By using different spectroscopic techniques such as electronic absorption, circular dichroism, nuclear magnetic resonance, and electron paramagnetic resonance, this study demonstrates that Cu(II) binding to the cleaved His111 site is highly dependent on Cu and proton concentrations. The imidazole group of His111 and its free NH_2 terminus emerge as the main anchoring sites for Cu(II) coordination, yielding very different complexes from those characterized for the intact His111 site in the full protein. Different Cu(II) coordination modes that could form with the alpha cleaved PrP^C under physiological conditions are identified and characterized. Overall, this study contributes to understand how alpha cleavage processing of PrP^C impacts its Cu(II) binding properties at His111. While the functional implications of Cu binding to the cleaved PrP^C remain to be discovered, proteolytic processing of PrP^C and its Cu binding features appear to be molecular events that might be strongly linked to its cellular function.

Received 12th September 2017,
Accepted 17th January 2018

DOI: 10.1039/c7dt03400h

rsc.li/dalton

Introduction

The cellular prion protein (PrP^C) is a monomeric glycoprotein of 208 amino acids attached to the cell membrane by a glycosylphosphatidylinositol (GPI) anchor.[1] PrP^C is highly expressed in the central nervous system and is mainly localized at the synapsis.[2] Since PrP^C is located in lipid rafts, it is proposed that it functions as a signalling transducer from the extracellular space to the interior of the cell.[3] Post-translational modifications of PrP^C, such as endoproteolytic cleavage events, have been linked to its potential role in cell signalling. The alpha-cleavage is the main proteolytic processing event of PrP^C, and it occurs even when the protein is not anchored to the lipid membrane.[4] Zinc-dependent members of the A-disintegrin-and-metalloproteinase (ADAM) family proteases have been proposed to engage in this cleavage.[5,6] The alpha-cleavage site is located at His111 in the human sequence,[5–9] producing two fragments: the N-terminal fragment N1, spanning residues 23–110; and the C-terminal fragment C1, which includes residues 111–231 with a free NH_2-terminus (Scheme 1).[9] The C1 fragment remains anchored to the membrane, representing 5 to 50% of the total PrP^C levels, depending on the brain region.[5,10]

Since the alpha-proteolytic cleavage breaks the region 106–126, which is key for the conversion of PrP^C into its infectious isoform PrP^{Sc},[2,11] the biological activity of the resulting fragments became an active area of research.[2,5,6,11,12] The

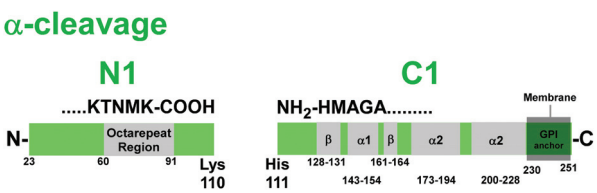

Scheme 1 Alpha-cleavage processing of PrP^C.

[a]Departamento de Química, Centro de Investigación y de Estudios Avanzados (Cinvestav), Mexico City, Mexico. E-mail: lilianaq@cinvestav.mx
[b]Max Planck Laboratory for Structural Biology, Chemistry and Molecular Biophysics of Rosario (MPLbioR, UNR-MPIbpC) and Instituto de Investigaciones para el Descubrimiento de Fármacos de Rosario (IIDEFAR, UNR-CONICET), Universidad Nacional de Rosario, Ocampo y Esmeralda, S2002LRK Rosario, Argentina

†Electronic supplementary information (ESI) available. See DOI: 10.1039/c7dt03400h

soluble N1 fragment plays a role in intercellular communication and neuroprotective functions, while its production also prevents neurotoxicity caused by amyloid beta oligomers involved in Alzheimer's disease.[5] On the other hand, the membrane-bound C1 fragment lacks the ability to fold into the pathogenic PrP^{Sc} isoform, and its increased levels relative to full length PrP^{C} were shown to exert protective effects against prion disease.[5,12]

Another important feature of PrP^{C} is that it binds copper *in vivo*.[13] PrP^{C} can coordinate up to six copper ions at its N-terminal region, and it has been proposed that it may play a role in copper transport.[14] Four Cu(II) ions bind at the octarepeat region spanning residues 60–91 and containing four PHGGGWGQ repeats,[15] while His96 and His111 are the anchoring sites for two Cu(II) ions.[16–18] Each histidine, His96 and His111, binds Cu(II) independently, involving the imidazol group and deprotonated amides from the peptide bonds that precede the His residue.[19,20] For the His111 site, these amide groups involve those of Met109, Lys110 and His111. These Cu coordination properties are found in the full-length prion protein; however, when PrP^{C} suffers endoproteolytic alpha-cleavage at the Lys110/His111 site, the protein lacks the amide groups that are known to participate in Cu coordination to the His111 site. Since alpha-cleavage is the main proteolytic event of PrP^{C}, and Cu binding is an important feature of this protein, it becomes relevant to explore how alpha-cleavage processing might impact the Cu(II) coordination properties of PrP^{C} at the His111 site. In this work, the hPrP(111–115) fragment, NH_2-HMAGA, was used as a model to study Cu(II) coordination to the C1 fragment using spectroscopic techniques such as UV/Vis absorption, circular dichroism (CD), electron paramagnetic resonance (EPR) and nuclear magnetic resonance (NMR). The roles of the N-terminal NH_2 group and His111 in Cu(II) coordination were evaluated by studying the acetylated peptide, Ac-HMAGA, and the H111A variant, NH_2-AMAGA, respectively.

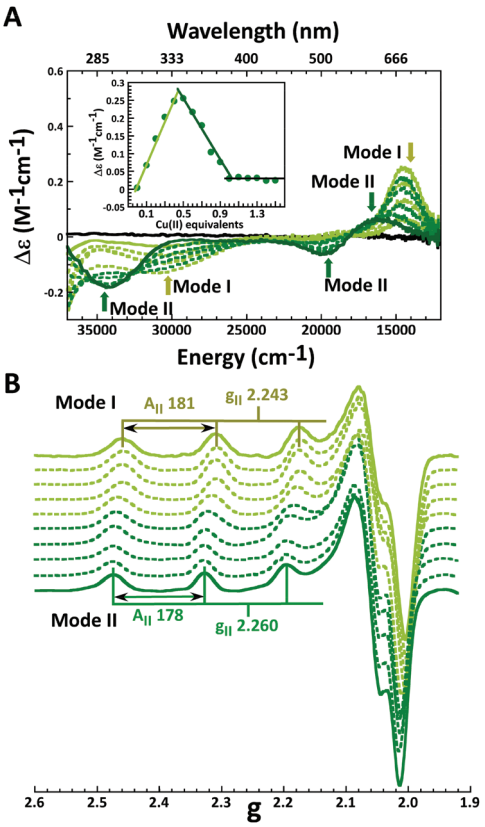

Fig. 1 Titration of the hPrP(111–115) fragment with Cu(II) as followed using CD (A) and EPR (B) at pH 7.5. (A) Dotted olive green lines correspond to the addition of 0.1 to 0.4 eq. of Cu(II) and the solid olive green line corresponds to the addition of 0.5 eq. Cu(II). Dotted dark green lines correspond to the addition of 0.6 to 0.9 eq. of Cu(II) and the solid dark green line corresponds to the addition of 1.0 eq. Cu(II). The inset in A shows the CD signal intensity at 14 451 cm^{-1} plotted as a function of the number of equivalents of Cu(II) added. EPR parameters for modes I and II were extracted from EPR simulations (Fig. S2 and Table S3†).

Results and discussion

hPrP(111–115): a model for Cu(II) coordination to C1 fragment

The peptide hPrP(111–115) with the sequence HMAGA and its free NH_2 group was used as a model for copper coordination to the C1 fragment that results from alpha-cleavage of PrP^{C}. The hPrP(111–115) fragment was titrated with Cu(II) at pH 7.5 and followed using UV-vis absorption (Fig. S1†), CD and EPR (Fig. 1). In the range of 0.1 to 0.5 equiv. of Cu(II), the CD spectra show the growth of a set of signals: a negative band with a high intensity at 43 000 cm^{-1} that corresponds to a NH_2 to Cu(II) ligand-to-metal charge transfer (LMCT) (Fig. S1†); a negative band at 30 600 cm^{-1} assigned to an imidazole π_1 to Cu(II) LMCT; and a positive ligand field transition at 14 400 cm^{-1} (Fig. 1A and Table S1†). Fig. 1B shows the titration followed using EPR, where all signals display $g_{II} > g_{\perp} > 2.0023$, and a large parallel hyperfine splitting (A_{II}), indicative of a tetragonal Cu(II) center with a ground state $d_{x^2-y^2}$.[21] At low equiv. of Cu(II), a set of signals with $g_{II} = 2.243$ and $A_{II} = 181 \times 10^{-4}$ cm^{-1} is observed (Fig. 1B and S2, Table S3†); it corresponds to a nitrogen rich coordination mode, named here mode I, and it can be associated with the species observed by CD, as described above. Given the observed LMCT signals, both, the NH_2 terminal group and the His residue, must participate in copper binding in mode I. The imidazole ring can coordinate Cu(II) by its N1 or N3, yielding distinct paramagnetic effects of Cu(II) on the relaxation rates of the protons Hε and Hδ.[22] Fig. 2A shows the broadening effect on both signals after the addition of a substochiometric amount (0.02 equiv.) of Cu(II). Proton spin–lattice relaxation rates of the imidazole protons Hε and Hδ were measured. Fig. 2B displays the fits for T_1 of Hε (gray) and Hδ (black) for the free peptide, and for the species with 0.02 equivalent of copper Hε (light green) and Hδ (dark green). Table S2† shows the parameters T_1, R_{1b}, R_{1p} and the distance for the protons Hε and Hδ to Cu(II). $\tau_M = 1/k_{off}$ was calculated using a fixed distance of 0.3 nm from Cu(II) to Hε[22] of His111, obtaining a value of 9.9 ms. A global correlation time τ_C of 0.4 ns was assumed.[23] Therefore, by NMR spec-

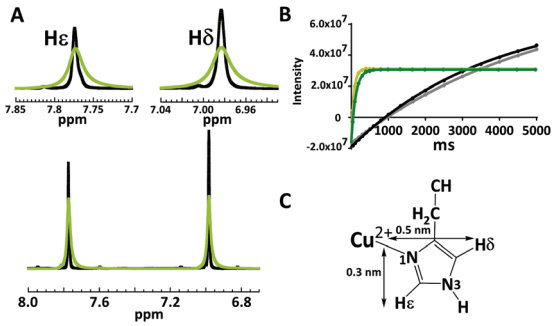

Fig. 2 (A) Overlaid 1D ^{1}H NMR spectra of hPrP(111–115) in the absence (black) and presence (green) of 0.02 equiv. of Cu(II); the insets show the broadening of Hε and Hδ signals from His111 imidazole upon the addition of the metal ion. (B) Fits from proton spin–lattice relaxation rates by 1D–IR experiments of Hε and Hδ of His111 imidazole in the absence and presence of Cu(II): free species correspond to Hε (gray) and Hδ (black), while bound species to 0.02 equiv. of Cu(II) correspond to Hε (light green) and Hδ (dark green). Scheme C represents Cu(II) binding to N1 from imidazole and the expected distances of Cu(II) to Hδ and Hε.

troscopy, it was possible to determine that N1 is the nitrogen from the His111 imidazole ring that is bound to Cu(II) (Fig. 2C) in the species named mode I. The EPR parameters of mode I are quite similar to those of the Cu(II)-(histamine)$_2$ complex, where the metal ion is coordinated by the NH_2 terminal and His imidazole groups of histamines, forming two chelate six-membered rings (Scheme 2).[24–26] Indeed, LMCT transitions from these ligands are observed for mode I, and its CD signals reach a maximum intensity at 0.5 equiv. of metal ions, after which the CD spectrum changes drastically (Fig. 1A, inset), consistent with mode I being a Cu(II)-(hPrP(111–115))$_2$ complex (Scheme 2). Previous potentiometric studies of Cu(II) binding to the HGG peptide actually support the formation of a 1 : 2 Cu : peptide complex where the NH_2 terminal and imidazole groups play an important role in metal coordination.[27,28]

A second species is observed from 0.6 to 1.0 equiv. of Cu(II) in the titration of hPrP(111–115) followed using CD. In fact, the intensity trace of the CD signal at 14 451 cm^{-1} (Fig. 1A, inset) reflects the formation of one species (mode I) from 0 to 0.5 equiv. of Cu(II), followed by its conversion into a second species (mode II) from 0.6 to 1.0 equiv. of Cu(II). This second species, named mode II, displays a negative LMCT band from NH_2 at 43 000 cm^{-1} (Fig. S1†); a negative band at 34 100 cm^{-1} that can be assigned to a deprotonated backbone amide N^{-} to Cu(II) LMCT, to an imidazole π_1 to Cu(II) LMCT, or a mixture of both; and two ligand field transitions: a positive one at 16 200 cm^{-1} and a negative one at 19 500 cm^{-1} (Fig. 1A and Table S1†). The EPR parameters associated with mode II are g_{II} = 2.260 and A_{II} = 178 × 10^{-4} cm^{-1} (Fig. 1B and S2, Table S3†), corresponding to a nitrogen rich equatorial coordination mode. Interestingly, the spin quantitation of the EPR titration shown in Fig. 1B clearly shows that mode II is likely to be a 1 : 2 Cu : peptide complex (Fig. S3†), although the formation of a 1 : 1 Cu : peptide complex with the participation of oxygen-based ligands to form a 3N1O species cannot be fully ruled out (Scheme 2). CD spectroscopic results suggest that the NH_2 terminal group, His111, and deprotonated backbone amides are plausible ligands for Cu(II) in mode II, although their role will be further investigated, as discussed below.

pH effect on Cu(II) coordination to the hPrP(111–115) peptide

The impact of pH on both coordination modes I and II was evaluated (Fig. 3). A pH titration of mode I, as followed using CD and EPR, shows that at high pH, mode I turns into a different species with EPR parameters g_{II} = 2.174 and A_{II} = 208 × 10^{-4} cm^{-1} (Fig. 3C and Table S3†) and a widely different CD spectrum (blue spectrum in Fig. 3A). This high pH species, named mode III, corresponds to a nitrogen rich coordination mode, likely involving the NH_2 terminal group and deprotonated backbone amides (*vide infra*). The pK_a associated with the conversion of mode I into mode III is 8.5 (Fig. 3B); thus, mode III may not be relevant at physiological pH. In contrast, the pH dependence of mode II displays two protonation equilibria (Fig. 3D and E). While mode II can also be converted into mode III with a pK_a of 8.4, at low pH mode II undergoes protonation to yield a species with EPR parameters g_{II} = 2.303 and A_{II} = 171 × 10^{-4} cm^{-1} (Fig. 3F and Table S3†), which are indicative of a more oxygen-rich equatorial coordination mode. This low pH species was named mode I′, since it still displays LMCT bands associated with NH_2 and His111 by CD (orange spectrum in Fig. 3D and Table S1†), suggesting that these groups may still be anchoring the metal ion, although the

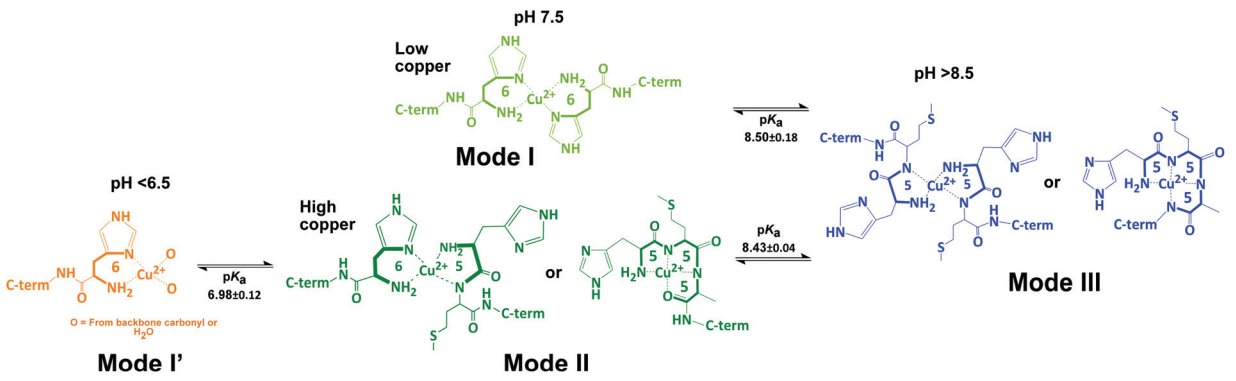

Scheme 2 Proposed coordination models for the Cu(II) complexes with hPrP(111–115) at different copper : peptide ratios and pH values.

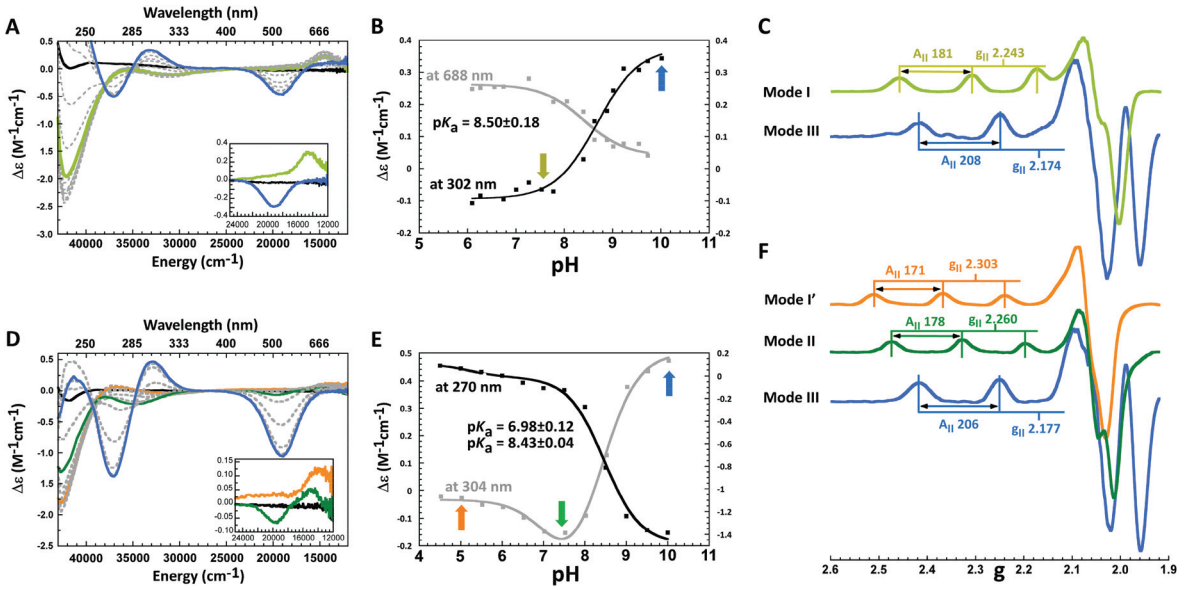

Fig. 3 pH titration of the Cu(II) complex with hPrP(111–115) at Cu(II):peptide ratios of 0.4 : 1.0 (A) and 1 : 1 (D). Traces for the changes in CD signal intensity at 14 535 cm^{-1} (688 nm, gray line) and 33 113 cm^{-1} (302 nm, black line) as a function of pH for the 0.4 : 1.0 Cu(II):peptide ratio are shown in (B); while traces at 32 895 cm^{-1} (304 nm, gray line) and 37 037 cm^{-1} (270 nm, black line) for the 1 : 1 Cu(II):peptide ratio are shown in (E); these traces were fit to models for one or two protonation equilibria to determine the associated pK_a values. EPR spectra at selected pH values of the titrations are shown in C and F, illustrating the set of signals associated with the coordination modes I (olive green, pH 7.5), I′ (orange, pH 5.0), II (dark green, pH 7.5) and III (blue, pH 10.0). EPR parameters for all coordination modes were extracted from EPR simulations (Fig. S2 and Table S3†).

equatorial coordination is completed by oxygen ligands from backbone carbonyl groups or water molecules (Scheme 2). The pK_a associated with the protonation of mode II to yield mode I′ is 6.9, and thus, at physiological pH, both coordination modes, I′ and II, would be formed upon Cu(II) binding to the C1 fragment.

The NH_2 group as an anchoring site for Cu(II) in hPrP (111–115)

In order to evaluate the participation of the N-terminal NH_2 group in Cu(II) coordination to the hPrP(111–115) fragment, a peptide with the same sequence but an acetylated N-terminus, Ac-HMAGA, was synthesized. A titration of the acetylated peptide, hPrP(Ac-111–115), with Cu(II) at pH 7.5 displays CD signals that indicate the formation of a 1 : 1 complex (data not shown). Fig. 4 shows the CD and EPR spectra of the complex with 1.0 equivalent of Cu(II), shown in purple. Clearly, the spectroscopic features of the acetylated complex are very different from those associated with mode I and mode II (Fig. 4), suggesting that the NH_2 group must be involved in such species. The CD spectrum of the acetylated complex Cu(II)-hPrP(Ac-111–115) shows a negative ligand field transition at 16 300 cm^{-1} and three LMCT bands: a positive band at 28 900 cm^{-1}, a negative band at 32 300 cm^{-1} and a positive band at 38 400 cm^{-1} (Fig. 4A and Table S1†), while the EPR parameters for this complex are g_{II} = 2.243 and $A_{II} = 156 \times 10^{-4}$ cm^{-1} (Fig. 4B). The spectroscopic features of the acetylated complex are almost identical to those observed for Cu(II) complexes involving a His residue and deprotonated amides from

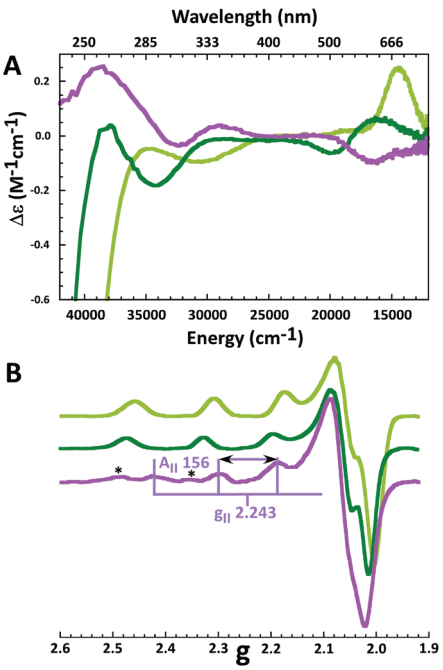

Fig. 4 Comparison of CD (A) and EPR (B) spectra of the Cu(II) complex with the acetylated peptide hPrP(Ac-111–115) with 1.0 equiv. of Cu(II) (purple) with those of the Cu(II) complexes with hPrP(111–115): mode I (with 0.5 equiv. of Cu, light green) and mode II (with 1.0 equiv. of Cu, dark green). All spectra were collected at pH 7.5. Asterisks indicate signals associated with copper in solution.

the backbone that follow the His in the sequence, with no involvement of an NH_2 group (Fig. S4†). Such a coordination mode has been observed for the Cu(II)-amylin complex and the complex with the K110P variant of hPrP(106–115), where Cu(II) can only recruit deprotonated amides towards the C-terminal (Fig. S4†).[20,29] Moreover, a pH titration of the acetylated complex shows no evidence for the formation of other species that would resemble mode I′ or mode III (Fig. S5†). Altogether, these results indicate that the acetylation of the NH_2 group in the hPrP(Ac-111–115) peptide yields a very different Cu(II) complex, as compared to the species formed with the peptide containing a free N-terminal. Thus, the NH_2 group must participate in all the species that result from Cu(II) coordination to hPrP(111–115).

His111 as an anchoring site for Cu(II) in hPrP(111–115)

In order to evaluate the role of His111 in Cu(II) coordination to hPrP(111–115), the variant hPrP(111–115 H111A) was synthesized. In this peptide, His111 was replaced by alanine while the NH_2 terminal group was kept intact. A titration of the peptide hPrP(111–115 H111A) with Cu(II) at pH 7.5 shows CD signals that saturate at 0.5 equiv. of Cu(II) (Fig. S6A† and the inset in Fig. 5A), indicating a 1 : 2 Cu(II):peptide molar stoichiometry. The CD spectrum of the Cu(II)-hPrP(111–115 H111A) complex (pink spectrum in Fig. 5A) displays one high intensity ligand field transition at 19 100 cm^{-1} and two LMCT transitions: a positive band at 32 400 cm^{-1} that can be assigned to a deprotonated backbone amide N^- to Cu(II) LMCT, and a high intensity negative band at 37 200 cm^{-1} that corresponds to a NH_2 to Cu(II) LMCT (Table S1†). Evidently, the CD spectrum of this complex is distinctly different from those associated with mode I and mode II, as characterized in hPrP(111–115) (Fig. 5A). Instead, the spectroscopic features of the Cu(II)-hPrP(111–115 H111A) complex are almost identical to those observed for the Cu(II)-hPrP(111–115) complex at high pH, namely mode III (blue spectra in Fig. 5). Furthermore, the EPR parameters for the Cu(II)-hPrP(111–115 H111A) complex (g_{II} = 2.178 and A_{II} = 212 × 10^{-4} cm^{-1}) are practically identical to those observed for mode III (g_{II} = 2.174 and A_{II} = 208 × 10^{-4} cm^{-1}) in the His containing peptide (Fig. 5B). A second species is observed in the EPR spectrum of the Cu(II)-hPrP(111–115 H111A) complex, which corresponds to the protonated complex, as it displays a pK_a of 7.37 (Fig. S6D†); it should be noted though that the protonated complex does not resemble any of the species observed for the His containing peptide, including modes I′ and II (Fig. S6C†). The protonated species observed in the pH titration of this Cu(II)-H111A complex likely correspond to 2N2O and 3N1O coordination modes involving the NH_2 group, deprotonated amides and oxygen based ligands such as backbone carbonyls or water molecules, as observed for multiglycine complexes that lack an imidazole moiety[24] (Fig. S6†). Overall, these results clearly indicate that His111 must be an anchoring site for Cu(II) coordination in the complexes described as mode I′, mode I and mode II, while the formation of mode III does not require the presence of His111. Based on the spectroscopic properties of mode III,

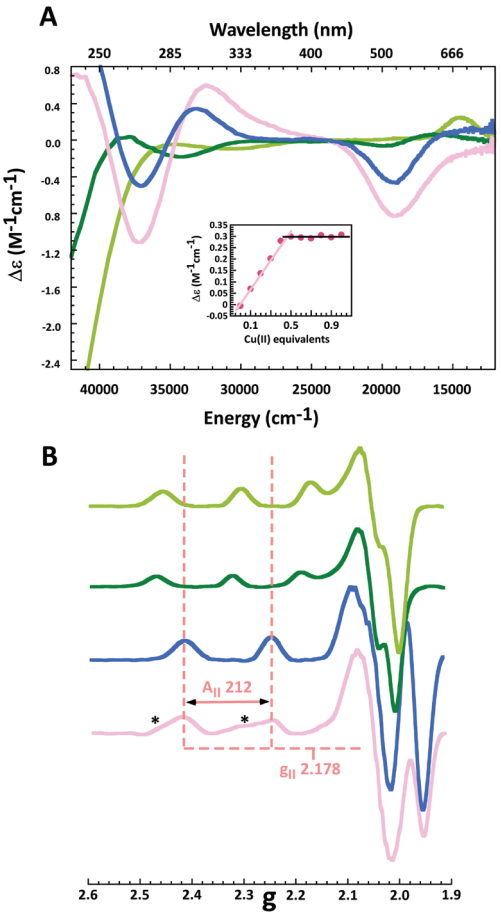

Fig. 5 Comparison of CD (A) and EPR (B) spectra of the Cu(II) complex with the variant hPrP(111–115 H111A) with 1.0 equiv. of Cu(II) at pH 7.5 (pink) with those of the Cu(II) complexes with hPrP(111–115): mode I (with 0.5 equiv. of Cu, light green), mode II (with 1.0 equiv. of Cu, dark green) and mode III (with 1.0 equiv. of Cu at pH 10.0, blue). The inset in A shows the growth of the CD signal intensity at 32 468 cm^{-1} plotted as a function of the number of equivalents of Cu(II), extracted from the titration of the H111A variant at pH 7.5 (Fig. S6A†). Asterisks in the EPR pink spectrum indicate signals associated with a protonated species.

its stoichiometry and spin quantitation (Fig. S3†), and the fact that His111 does not participate in this coordination mode, it is proposed that in mode III Cu(II) is coordinated by two NH_2 terminal groups and two deprotonated amides from two peptide units, yielding a stable set of 5-membered chelate rings (Scheme 2).

It is important to note that, while the EPR spectrum of mode III is quite similar to 4N complexes with three deprotonated amides (as shown for the 1 : 1 model in Scheme 2), the stoichiometry and spin quantitation of the complex strongly support the model of a 1 : 2 Cu : peptide complex. It is likely that the deprotonation of a second and a third amide group to yield the 1 : 1 complex may not be favored by the steric effect of having His and Met side chains on the same side of the 4N plane. In fact, in other hPrP binding sites, it has been noted that having bulky side chains impacts the pK_a of their amide groups when it comes to the formation of a square planar

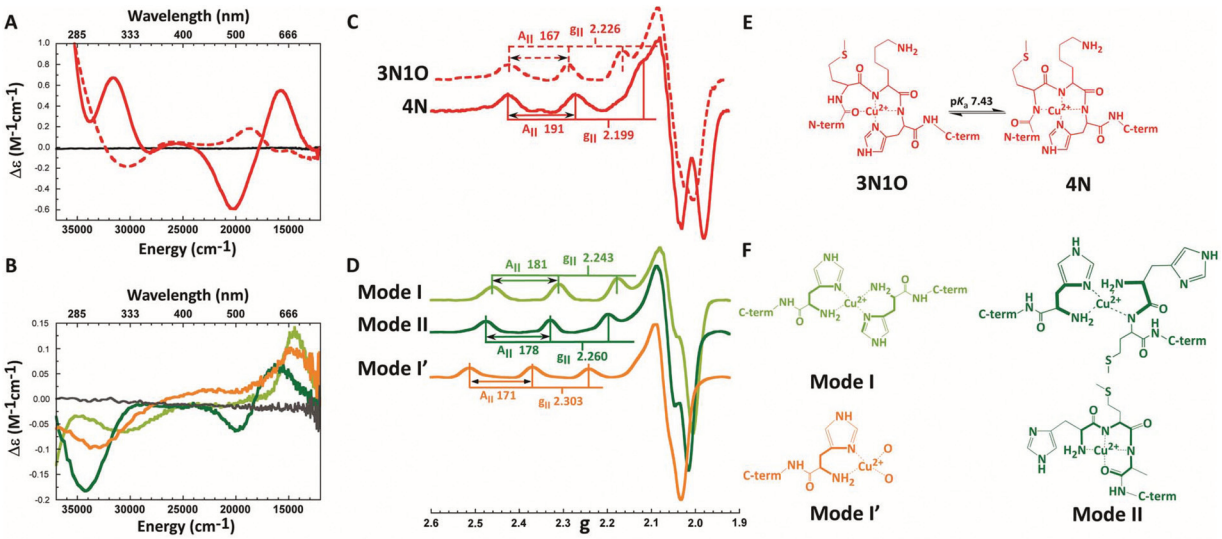

Fig. 6 Comparison of the spectroscopic features of Cu(II) bound to the intact His111 site in the full protein (as modeled by the PrP fragment 106–115, A&C) with those characterized in this study, using the PrP fragment 111–115 to model the C1 fragment resulting from alpha cleavage of PrP (B&D). The proposed coordination modes resulting from Cu(II) binding to hPrP(111–115) at different pH values and copper : peptide ratios (F) are clearly distinct from those observed in the intact His111 site (E).

Cu(II) complex with a 4N coordination mode.[30] Moreover, this steric effect might also play a role in favoring the 1 : 2 complex for mode II over the 1 : 1 Cu : peptide complex with a 4N equatorial coordination mode (Scheme 2).

Cu(II) coordination modes at the His111 site: impact of alpha cleavage processing

The spectroscopic study of Cu(II) coordination to hPrP (111–115), as a model for the C1 fragment, has led to the identification of four different species, termed mode I′, mode I, mode II and mode III. The study of the acetylated peptide clearly indicates that the NH_2 group participates in all species, while the study of the H111A variant shows that His111 is the anchoring site in mode I′, mode I and mode II, but it does not participate in mode III. Altogether, based on these spectroscopic results, structural models for the species formed upon coordination of Cu(II) to hPrP(111–115) are shown in Scheme 2.

While modes I′, I, and II would be physiologically relevant, mode III would not, as it forms at high pH. It is important to highlight that the spectroscopic features for modes I′, I, and II are different from those observed for Cu(II) bound to an intact His111 site (Fig. 6). The His111 site before cleavage has been modelled by the hPrP(106–115) fragment with an acetylated N-terminus and an amidated C-terminal.[20] Cu(II) coordination to the intact His111 site at pH 7.5 yields two coordination modes, 3N1O and 4N, with resolved spectroscopic features as shown in Fig. 6A and C. In both cases, Cu(II) coordination involves His111 and deprotonated amides that precede the His residue in the sequence (Fig. 6E). In contrast, the free NH_2-terminal group and His111 emerge as the main anchoring sites for Cu(II) coordination in the cleaved site, as modelled by hPrP(111–115) (Fig. 6F).

Thus, upon alpha cleavage processing of PrP^C, the cleaved His111 site contains a free NH_2 group that significantly impacts the coordination chemistry of this site.

Finally, it is important to note that the coordination mode I (and possibly mode II as well) that forms upon Cu(II) coordination to hPrP(111–115) at pH 7.5 has a 1 : 2 Cu to peptide stoichiometry. Since the C1 fragment of PrP^C remains anchored to the extracellular membrane after alpha cleavage processing, the formation of species such as mode I would only be possible if two molecules of cleaved PrP^C are located in close proximity in the membrane or lipid raft. While it is not clear if this would be feasible in neurons, it is important to highlight that dimerization of membrane bound proteins plays important roles in cell signalling. In particular, examples of copper-mediated dimerization of membrane bound proteins are found for the amyloid precursor protein and a receptor for vascular endothelial growth factors (VEGFs); in both cases, dimerization is proposed to be involved in cell signalling cascades.[31,32] Thus, if the formation of Cu(II) coordination modes I and II with two molecules of cleaved PrP^C were feasible *in vivo*, this Cu–protein interaction might be relevant for the proposed cell signalling function of PrP^C.

Conclusions

In summary, we report here the coordination of Cu(II) to a peptide that models the membrane-anchored C1 fragment resulting from endoproteolytic alpha cleavage of PrP^C. Our study demonstrates that Cu(II) binding to the cleaved His111 site leads to different coordination modes that would be

physiologically relevant (Fig. 6F), and are dependent on copper and proton concentrations. The fact that the C1 fragment of PrP^C remains anchored to the extracellular membrane and is exposed to important fluctuations in copper concentration during synaptic transmission underscores the importance of the copper chemistry described here. The Cu(II)-hPrP(111–115) complexes identified in this work could be formed under physiological conditions when PrP^C suffers endo-proteolytic alpha cleavage.

While the functional implications of Cu binding to the membrane anchored C1 fragment of PrP^C remain to be discovered, proteolytic processing of PrP^C and its Cu binding features appear to be molecular events that might be strongly linked. Indeed, Cu(II) binding to PrP^C suppresses its alpha-cleavage,[6] and in turn, this proteolytic processing would significantly impact the Cu coordination properties of the protein, as demonstrated in this study. A further understanding of how these events impact the conformation of the membrane-anchored C-terminal region of the prion protein will provide insight into their roles in the structure–function relationship of this intriguing protein.

Experimental

Reagents

9-Fluorenylmethoxycarbonyl (Fmoc) protected amino acids, Fmoc Rink amide AM resin and ethyl (hydroxyimino)-cyano-acetate (oxyme pure) were obtained from Novabiochem. The reagents and solvents *N*,*N*-dimethylformamide (DMF), *N*,*N*-diisopropylethylamine (DIEA), pyridine, *N*,*N*-diisopropyl-carbodiimide (DIC), trifluoroacetic acid (TFA), trisisopropyl-silane (TIS), ethanedithiol (EDT), acetonitrile (HPLC grade) and piperidine were obtained from Sigma. Water was purified to a resistivity of 18 MΩ cm^{-1} using a Millipore gradient de-ionizing system. Deuterium oxide and deuterated 2-(*N*-morpholino)ethanesulfonic acid (MES) buffer were purchased from Sigma.

Peptide synthesis and purification

The peptides hPrP(111–115) with the sequence NH_2-HMAGA, hPrP(111–115 H111A) with the sequence NH_2-AMAGA and hPrP(Ac-111–115) with the sequence Ac-HMAGA were synthesized by solid-phase synthesis and Fmoc strategy, using Fmoc-Rink amide resin.[33,34] For hPrP(111–115) and hPrP (111–115 H111A) their carboxylic terminals were amidated, and for hPrP(Ac-111–115) the N-terminal was acetylated and its carboxylic terminal was amidated. The crude peptide was purified by HPLC using a semi-preparative C18 reversed phase column. Peptide purity was determined by analytical HPLC and was found to be >95%. The molecular weight of the peptide was determined by Electrospray Ionization Mass Spectrometry (ESI-MS), and the purified product presented the expected molecular mass. The lyophilized pure peptides were stored in a desiccator until further use.

Preparation of samples

Peptide solutions were prepared in a mixture of 20 mM 2-(*N*-morpholino)ethanesulfonic acid (MES) buffer and 20 mM *N*-ethylmorpholine (NEM) buffer. The molar absorption coefficient for each peptide at 214 nm was determined in this buffer mixture by calibration curves using a microbalance (Mettler-Toledo XP26); for hPrP(111–115) ε = 9.038 mM^{-1} cm^{-1}. Final peptide concentrations in each sample were determined by absorption spectroscopy and were of the order of 0.5 mM. For the pH titrations, the pH was varied every 0.5 pH units by adding the necessary volume of NaOH or HCl solutions, and it was followed using circular dichroism spectroscopy. Peptide samples for EPR spectroscopy were prepared in the same buffer mixture with 50% glycerol to achieve adequate glassing. The addition of glycerol has no effect on the structure of the Cu(II)-peptide complexes, as evaluated by circular dichroism spectroscopy for all buffer solutions and pH values used in this study. For 1D–1R experiments the sample was prepared in 100% deuterium oxide and 20 mM of deuterated MES buffer with a final concentration of 0.3 mM. In each case the pH was adjusted to 7.5 with NaOD in D_2O.

Spectroscopic characterization

UV-visible absorption and circular dichroism (CD) spectroscopy. Room temperature absorption spectra were recorded using an Agilent 8453 diode array spectrometer and CD spectra were acquired using a Jasco J-815 CD spectropolarimeter at room temperature. A 1 cm path length quartz cell was used for recording spectra between 230 and 830 nm with sampling points every 2 nm and a scanning speed of 100 nm min^{-1}.

EPR spectroscopy. X-band EPR spectra were collected using an EMX Plus Bruker system with an ER 041 XG microwave bridge and an ER 4102ST cavity. The following conditions were used: microwave frequency, 9.4 GHz; microwave power, 10 mW; modulation amplitude, 5 G; modulation frequency, 100 kHz; time constant, 327 ms; conversion time, 82 ms; and averaging over 6 scans. EPR spectra were recorded at 150 K using an ER4131VT variable temperature nitrogen system. The spin quantitation was done by comparing double integrals of each sample to that of a 1 mM $CuSO_4$ standard aqueous solution, which was run in parallel in the same quartz tube, for each experiment.

NMR spectroscopy. NMR spectra were acquired using a Bruker 600 MHz Avance II instrument equipped with a cryogenically cooled triple resonance $^1H(^{13}C/^{15}N)$ TCl probe at 298 K. Chemical shifts were referenced to DSS as an internal standard. Proton spin–lattice relaxation rates were measured with the standard inversion recovery (1D–IR) pulse sequence.[35,36] The T_1 values were determined by a three-parameter fit of peak intensities to the following equation:

$$I(t) = I_0[1 - (1 + B)\exp(-t/T_1)]$$

where B is a variable parameter that considers non-ideal magnetization whose value is less than unity. The paramagnetic

contributions of Cu(II) to the spin–lattice relaxation rate, R_{1p}, were calculated according to[37]

$$R_{1p} = R_{1obs} - p_f R_{1free} = p_b / R^{-1}{}_{1b} + \tau_M$$

where f and b refer to the free and metal-bound states, respectively, the p values are fractional populations of the peptide, R_{1free} and R_{1b} are the spin–lattice relaxation rates in the two environments, and τ_M (the inverse of the off-rate kinetic constant) is the residence time of the peptide in the metal coordination sphere. R_{1b} ($1/T_{1b}$) is accounted for by the Solomon equation describing the dipole–dipole nuclear spin–electron spin interaction, here reported for systems with $S = 1/2$:[37,38]

$$R_{1b} = 1/10\ (\mu_0/4\pi)^2(2\hbar^2\gamma_I{}^2\gamma_S{}^2/r^6)[(t_C/1 + (\omega_I - \omega_S)^2\tau_C{}^2) + (3\tau_C/1 + \omega_I{}^2\tau_C{}^2) + (6\tau_C/1 + (\omega_I - \omega_S)^2\tau_C{}^2)]$$

where μ_0 is the permeability of vacuum, γ_I and γ_S are the nuclear and electron magnetogyric ratios, respectively, $\hbar$ is the reduced Planck constant, ω_I and ω_S are the nuclear and electron Larmor frequencies, respectively, r is the proton–metal distance, and τ_C is the effective correlation time. Acquisition, processing and visualization of the NMR spectra were performed using TOPSPIN 3.2 (Bruker) and CcpNmr Analysis 2.4.2.[39]

Conflicts of interest

There are no conflicts to declare.

Acknowledgements

This research was funded by the National Council for Science and Technology in Mexico (CONACYT) through Grant No. 221134 and 128411 and a graduate fellowship to C. S. L. The authors would also like to thank Dr Marco C. Miotto and Dr Andres Binolfi for assistance in the acquisition of NMR data and valuable contributions to the discussion of the results and Q. Atenea Villegas and M. en C. Yanahi Posadas for assistance with peptide synthesis and purification of the NH_2-AMAGA peptide and for useful discussions.

References

1 R. Linden, V. R. Martins, M. A. M. Prado, M. Cammarota, I. Izquierdo and R. R. Brentani, *Physiol. Rev.*, 2008, **88**, 673–728.
2 J. Liang and Q. Kong, *Prion*, 2012, **6**, 453–460.
3 C. L. Haigh, V. A. Lewis, L. J. Vella, C. L. Masters, A. F. Hill, V. A. Lawson and S. J. Collins, *Cell Res.*, 2009, **19**, 1062–1078.
4 A. R. Walmsley, N. T. Watt, D. R. Taylor, W. S. Perera and N. M. Hooper, *Mol. Cell. Neurosci.*, 2009, **40**, 242–248.
5 H. C. Altmeppen, B. Puig, F. Dohler, D. K. Thurm, C. Falker, S. Krasemann and M. Glatzel, *Am. J. Neurodegener. Dis.*, 2012, **1**, 15–31.
6 A. J. McDonald, J. P. Dibble, E. G. Evans and G. L. Millhauser, *J. Biol. Chem.*, 2014, **289**, 803–813.
7 A. Jiménez-Huete, P. M. J. Lievens, R. Vidal, P. Piccardo, B. Ghetti, F. Tagliavini, B. Frangione and F. Prelli, *Am. J. Pathol.*, 1998, **153**, 1561–1572.
8 A. Mangé, F. Béranger, K. Peoc'h, T. Onodera, Y. Frobert and S. Lehmann, *Biol. Cell*, 2004, **96**, 125–132.
9 S. G. Chen, D. B. Teplow, P. Parchi, J. K. Teller, P. Gambetti and L. Autilio-Gambetti, *J. Biol. Chem.*, 1995, **270**, 19173–19180.
10 C. L. Haigh and S. J. Collins, *Neural Regen. Res.*, 2016, **11**, 238–239.
11 H. C. Altmeppen, J. Prox, B. Puig, F. Dohler, C. Falker, S. Krasemann and M. Glatzel, *FEBS J.*, 2013, **280**, 4338–4347.
12 L. Westergard, J. A. Turnbaugh and D. A. Harris, *J. Biol. Chem.*, 2011, **286**, 44234–44242.
13 D. R. Brown, K. Qin, J. W. Herms, A. Madlung, J. Manson, R. Strome, P. E. Fraser, T. Kruck, A. v. Bohlen, W. Schulz-Schaeffer, A. Giese, D. Westaway and H. Kretzschmar, *Nature*, 1997, **390**, 684–687.
14 G. L. Millhauser, *Annu. Rev. Phys. Chem.*, 2007, **58**, 299–320.
15 M. Chattopadhyay, E. D. Walter, D. J. Newell, P. J. Jackson, E. Aronoff-Spencer, J. Peisach, G. J. Gerfen, B. Bennett, W. E. Antholine and G. L. Millhauser, *J. Am. Chem. Soc.*, 2005, **127**, 12647–12656.
16 C. E. Jones, M. Klewpatinond, S. R. Abdelraheim, D. R. Brown and J. H. Viles, *J. Mol. Biol.*, 2005, **346**, 1393–1407.
17 A. R. Thompsett, S. R. Abdelraheim, M. Daniels and D. R. Brown, *J. Biol. Chem.*, 2005, **280**, 42750–42758.
18 M. Klewpatinond, P. Davies, S. Bowen, D. R. Brown and J. H. Viles, *J. Biol. Chem.*, 2008, **283**, 1870–1881.
19 C. Hureau, L. Charlet, P. Dorlet, F. Gonnet, L. Spadini, E. Anxolabéhère-Mallart and J. J. Girerd, *J. Biol. Inorg. Chem.*, 2006, **11**, 735–744.
20 L. Rivillas-Acevedo, R. Grande-Aztatzi, I. Lomelí, J. E. García, E. Barrios, S. Teloxa, A. Vela and L. Quintanar, *Inorg. Chem.*, 2011, **50**, 1956–1972.
21 G. Hanson and L. Berliner, *High Resolution EPR. Applications to metalloenzymes and metals in medicine*, Springer, 2009.
22 E. Gaggelli, H. Kozlowski, D. Valensin and G. Valensin, *Mol. BioSyst.*, 2005, **1**, 79–84.
23 A. Binolfi, E. E. Rodriguez, D. Valensin, N. D'Amelio, E. Ippoliti, G. Obal, R. Duran, A. Magistrato, O. Pritsch, M. Zweckstetter, G. Valensin, P. Carloni, L. Quintanar, C. Griesinger and C. O. Fernandez, *Inorg. Chem.*, 2010, **49**, 10668–10679.
24 H. Kozlowski, W. Bal, M. Dyba and T. Kowalik-Jankowska, *Coord. Chem. Rev.*, 1999, **184**, 319–346.
25 C.-C. Su and T.-Y. Chang, *J. Coord. Chem.*, 1994, **31**, 79–92.

26 I. Sóvágó, C. Kállay and K. Várnagy, *Coord. Chem. Rev.*, 2012, **256**, 2225–2233.
27 A. Yokoyama, H. Aiba and H. Tanaka, *Bull. Chem. Soc. Jpn.*, 1974, **47**, 112–117.
28 A. Demaret, A. Ensuque and G. Lapluye, *J. Chim. Phys.*, 1983, **80**, 475–480.
29 C. Sánchez-López, R. Cortés-Mejía, M. C. Miotto, A. Binolfi, C. O. Fernández, J. M. Del Campo and L. Quintanar, *Inorg. Chem.*, 2016, **55**, 10727–10740.
30 L. Quintanar, L. Rivillas-Acevedo, R. Grande-Aztatzi, C. Z. Gómez-Castro, T. Arcos-López and A. Vela, *Coord. Chem. Rev.*, 2013, **257**, 429–444.
31 F. Baumkotter, N. Schmidt, C. Vargas, S. Schilling, R. Weber, K. Wagner, S. Fiedler, W. Klug, J. Radzimanowski, S. Nickolaus, S. Keller, S. Eggert, K. Wild and S. Kins, *J. Neurosci.*, 2014, **34**, 11159–11172.
32 J. F. Gaucher, M. Reille-Seroussi, N. Gagey-Eilstein, S. Broussy, P. Coric, B. Seijo, M. B. Lascombe, B. Gautier, W. Q. Liu, F. Huguenot, N. Inguimbert, S. Bouaziz, M. Vidal and I. Broutin, *PLoS One*, 2016, **11**, e0167755.
33 K. J. Jensen, P. T. Shelton and S. L. Pedersen, *Peptide synthesis and applications*, Humana Press, New York, 2 edn., 2013.
34 R. Subirós-Funosas, R. Prohens, R. Barbas, A. El-Faham and F. Albericio, *Chem. – Eur. J.*, 2009, **15**, 9394–9403.
35 E. Gaggelli, F. Bernardi, E. Molteni, R. Pogni, D. Valensin, G. Valensin, M. Remelli, M. Luczkowski and H. Kozlowski, *J. Am. Chem. Soc.*, 2005, **127**, 996–1006.
36 J. G. Huber, J.-M. Moulis and J. Gaillard, *Biochemistry*, 1996, **35**, 12705–12711.
37 I. Bertini and C. Luchinat, *Coord. Chem. Rev.*, 1996, **150**, 1–292.
38 I. Solomon, *Phys. Rev.*, 1955, **99**, 559–565.
39 W. F. Vranken, W. Boucher, T. J. Stevens, R. H. Fogh, A. Pajon, M. Llinas, E. L. Ulrich, J. L. Markley, J. Ionides and E. D. Laue, *Proteins*, 2005, **59**, 687–696.